Research Article

Zaamoune Faiza* and Menacer Tidjani

The behavior of hidden bifurcation in 2D scroll via saturated function series controlled by a coefficient harmonic linearization method

https://doi.org/10.1515/dema-2022-0211
received September 28, 2021; accepted February 16, 2023

Abstract: In this article, the behavior of hidden bifurcation in a two-dimensional (2D) scroll via saturated function series controlled by the coefficient harmonic linearization method is presented. A saturated function series approach for chaos generation. The systematic saturated function series methodicalness improved here can make multi-scroll and grid scroll chaotic attractors from a 3D linear autonomous system with a plain saturated function series supervisor. We have used a hidden bifurcation method in grid scroll., where the method of hidden bifurcation presented by Menacer, et al. in (2016) for Chua multi-scroll attractors. This additional parameter, which is absent from the initial problem, is perfectly adapted to unfold the structure of the multispiral chaotic attractor. The novelty of this article is twofold: first, the saturated function series model for hidden bifurcation in a $2-D$ scroll; and second, the control of hidden bifurcation behavior by the value of the harmonic coefficient k_3.

Keywords: hidden bifurcation, harmonic linearization, 2D scroll, saturated function series

MSC 2020: 39A21, 39A28, 39A33

1 Introduction

During precedent and until now, the generation of multispiral chaotic attractors has been extensively examined due to their hopeful applications in manifold real-world technologies. Few techniques have been suggested, like linear and nonlinear modulating functions and in electronic circuits (saturated circuits, etc.), for generating multispiral chaotic attractors see [1–3]. The issue of hidden oscillations in nonlinear control systems forces us to improvise a novel approximation of nonlinear oscillation theory. Meanwhile, during the initial institution and evolution of the theory of nonlinear oscillations in the first half of the twentieth century broad attention was given to the analysis and composite of oscillating systems, for which the solution of existing problems of oscillating ranks was not too uneasy [4].

The construction itself of many systems was such that they had oscillating solutions, the nature of which was almost clear. The rise in these systems' periodic solutions was visible by numerical analysis when the numerical integration procedure of the trajectories permitted one to track from the little neighborhood of equilibrium to a periodic trajectory [5,6]. A self-excited attractor's basin of attraction interferes with the neighborhood of an equilibrium point, whereas a hidden attractor's basin of attraction does not

* **Corresponding author: Zaamoune Faiza,** Department of Mathematics, University Mohemed Khider Biskra, Biskra, Algeria, e-mail: f.zaamoune@univ-biskra.dz
Menacer Tidjani: Department of Mathematics, University Mohemed Khider Biskra, Biskra, Algeria

intersect with the small neighborhoods of any equilibrium points, making it hard to find. The hidden attractors are important in engineering applications [1,7–15]. Though most multi-spirals generations are have been known for many years, it is only recently that they have been studied underneath the area of bifurcation theory [14]. In all the multispirals previously familiar, the number of spirals (or scrolls) is a fixed integer, whereas it depends on one or more discrete parameters after the rapid development in more than a decade. In [14], the authors modified the model of discrete parameters by producing hidden bifurcations and generating multispirals.

Thus, hidden bifurcation theory is instituted based on the hidden attractor theory introduced by Leonov et al. [8,10]. In this work, the focus is on the study of paradigm hidden bifurcation in 2D grid scroll chaotic attractors generated by saturated function series. In the work of Chen et al., a saturated function series was suggested for generating multispiral chaotic attractors, including 1D n-scroll, 2D $n \times m$-grid scroll, and 3D $n \times m \times l$-grid scroll chaotic attractors [9]. Additionally, in order to find the hidden bifurcations, we fixed p_1, p_2, and q_1, q_2 and introduce the new control parameter ε in the nonlinear part, governed by a homotopy parameter ε while keeping p_1, p_2, and q_1, q_2 constant. The parameter ε varies between 0 and 1, indicating that when it takes the value 0, the non-linear part of the system (1-2-3) is unpaired and an attractor in the form of a cycle is obtained, whereas when it takes the value 1, the attractor of the original system (1-2-3) is found to be, with a number of spirals, $m = (p_1 + q_1 + 2) * (p_2 + q_2 + 2)$. Between these two values of ε, the number of spirals is increased in direct proportion to ε.

The aspects of this article are as follows: (i) the study of hidden bifurcation of 2D $n \times m$-grid scroll chaotic attractors via saturated function series with a method based on a homotopy parameter ε while conserving the number of scrolls constant [14]; the novel idea of controlling the parameter k_3 harmonic linearization method the spirals in $2 - Dn \times m$ grid scroll chaotic attractors via saturation function series is introduced, which is related to the behavior of spirals while taking one and two values of the parameter k_3.

This article is organized as follows: in Section 2, we first present the model of 2D $n \times m$-grid scroll chaotic attractors generated by saturated function series proposed in [9], then we introduce the analytical-numerical method for hidden attractor localization proposed by Leonov [10], Leonov and Kuznetsov [11], and finally we introduce the Poincare map for harmonic linearization in vector case. Section 3 is devoted to the localization of hidden bifurcations of $2 - Dn \times m$ grid- scroll chaotic attractors via saturated function series. In addition, we presented a new idea about controlling the parameter k_3 harmonic linearization method of behavior of the spirals, and we are given the results of the numerical bifurcation of the analysis. Finally, in Section 4, a brief conclusion is drawn.

2 Analytical-numerical method for double-spiral chaotic attractors from saturated function series

2.1 Double-spiral attractors generated via a saturated function series

In the following, to create a 2D $n \times m$-grid scroll chaotic attractors [1], a saturated function series as a controller is added to system 1 leading to [9], and see the Figure 1,

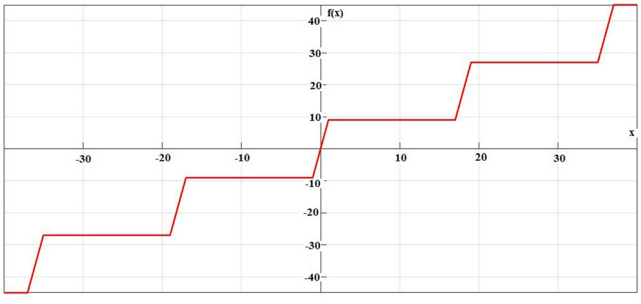

Figure 1: Graph of saturated function series for $k = 9$, $h = 18$.

$$\begin{cases} \dot{x} = y - \dfrac{d_2}{b} g(y;\, k_2;\, h_2;\, p_2;\, q_2) \\ \dot{y} = z \\ \dot{z} = -ax - by - cz + d_1 f(x;\, k_1;\, h_1;\, p_1;\, q_1) + d_2 g(y;\, k_2;\, h_2;\, p_2;\, q_2), \end{cases} \tag{1}$$

where

$$f(x;\, k_1;\, h_1;\, p_1;\, q_1) = \begin{cases} y_1 & \text{if } x > q_1 h_1 + 1 \\ y_2 & \text{if } |x - i h_1| \le 1, -p_1 \le i \le q_1 \\ y_3 & \text{if } i h_1 + 1 < x < (i+1) h_1 - 1 \quad \text{and} \quad -p_1 < i < q_1 - 1 \\ y_4 & \text{if } x < -p_1 h_1 - 1, \end{cases} \tag{2}$$

$y_1 = (2q_1 + 1)k_1$, $y_2 = k_1(x - ih_1) + 2ik_1$, $y_3 = (2i + 1)k_1$, and $y_4 = -(2q_1 + 1)k_1$,

$$g(y;\, k_2;\, h_2;\, p_2;\, q_2) = \begin{cases} y_1 & \text{if } y > q_2 h_2 + 1 \\ y_2 & \text{if } |y - i h_2| \le 1, -p_2 \le i \le q_2 \\ y_3 & \text{if } i h_2 + 1 < y < (i+1) h_2 - 1 \quad \text{and} \quad -p_2 < i < q_2 - 1 \\ y_4 & \text{if } x < -p_2 h_2 - 1, \end{cases} \tag{3}$$

$y_1 = (2q_2 + 1)k_2$, $y_2 = k_2(y - ih_2) + 2ik_2$, $y_3 = (2i + 1)k_2$, and $y_4 = -(2q_2 + 1)k_2$.

The parameters p_1, q_1, p_2, q_2, h_1, h_2, and k_1, k_2 are integers and a, b, c, d_1, and d_2 are real numbers. So, the number m of scrolls is defined as follows:

$$m = (p_1 + q_1 + 2) * (p_2 + q_2 + 2).$$

For $k_1 = k_2 = 50$, $h_1 = h_2 = 100$, $p_1 = p_2 = 1$, and $q_1 = q_2 = 0$, a nine-scroll attractor is generated as the verged attractor of system (1-2-3), see Figure 2.

2.1.1 Attraction basin of the nine spirals attractors

For our system (1-2-3), we have a $(2p_1 + 2q_1 + 3) * (2p_2 + 2q_2 + 3)$ equilibrium point situated along the y-axis, which can be categorized into two different sets as follows:

$$N_y = \left\{ -\frac{(2p_1 + 1)d_2k_2}{b}, \frac{(-2p_1 + 1)d_2k_2}{b}, \ldots, \frac{(2q_2 + 1)d_2k_2}{b} \right\}$$

$$M_y = \left\{ -\frac{p_2k_2d_2(h_2 - 2)}{k_2d_2 - b}, \frac{(-p_2 + 1)k_2d_2(h_2 - 2)}{k_2d_2 - b}, \ldots, \frac{q_2k_2d_2(h_2 - 2)}{k_2d_2 - b} \right\}.$$

For all equilibria in two sets N_y and M_y are saddle points (for more information see [9] (Lü 2007)).

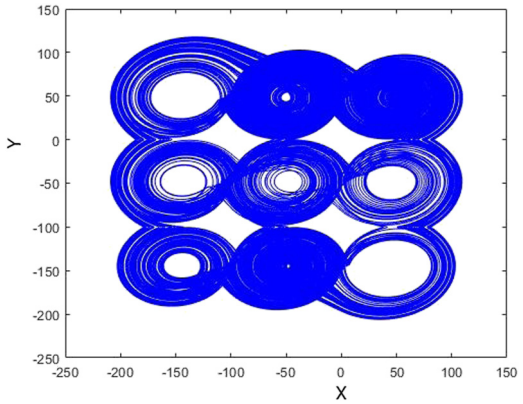

Figure 2: Two-directional 3 × 3-grid scroll chaotic attractors for $k_1 = k_2 = 50$, $h_1 = h_2 = 100$, $p_1 = p_2 = 1$, $q_1 = q_2 = 0$.

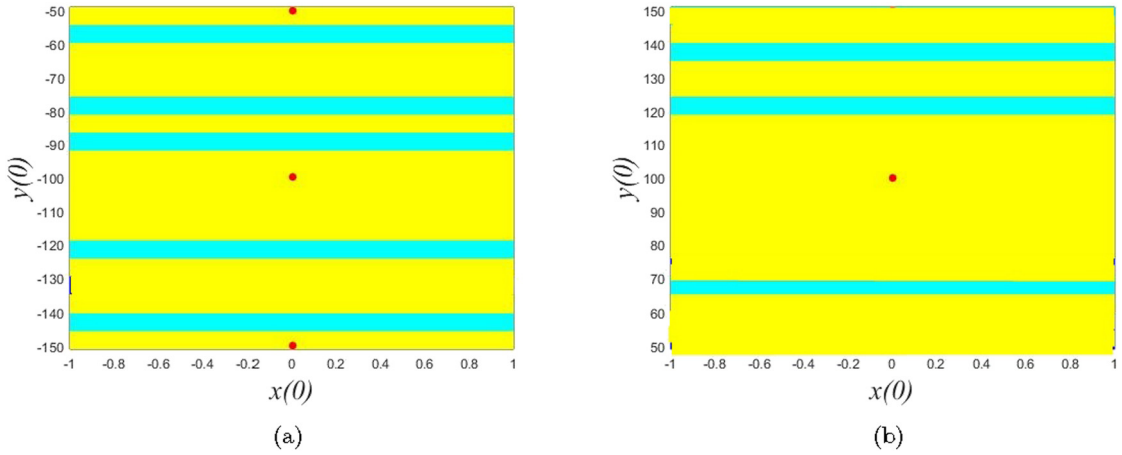

Figure 3: The attraction basin of 9 spirals attractors. (a) Attraction basin attractors cross section passing through four equilibrium points (0, −50, 0), (0, −100, 0), (0, −150, 0) and (b) attraction basin zooming in around (0, 100, 0) equilibrium point.

In this obstacle, we took $p_1 = p_2 = 1$ and $q_1 = q_2 = 0$, so we have 25 equilibrium points that are unstable points. Since all of the points in our system are unstable, we do not have any hidden attractors, which is why we are interested in the attraction basin. We took some points as we saw that the same outcomes appeared in all figures. The motion starting in these initial state regions is depicted by cyan color, which will diverge from equilibrium points, while the yellow regions denote the attraction basin of chaotic attractors (Figure 3).

2.2 Analytical-numerical method for attractors localization

Twelve years ago, Leonov [10], Leonov and Kuznetsov [11,13], proposed an effective method for the numerical localization of hidden attractors in multidimensional dynamical systems. They improve this method, especially for Chua attractors. In 2016, the method developed by Menacer et al. to discover hidden bifurcations in the multispiral Chua attractor was published. For the search of periodic solution close to harmonic oscillation, we consider a coefficient of harmonic linearization k_3 at like the matrix G_0 as:

$$\frac{\mathrm{d}x}{\mathrm{d}t} = Gx + \delta\Psi(\kappa^T x), \quad x \in \mathbb{R}^3, \tag{4}$$

where G is a constant $(n \times n)$ matrix, δ and κ are constant n-dimensional vectors, T is a transposition operation, $\Psi(\iota)$ is a continuous piecewise-differentiable vector-function, and $\Psi(0) = 0$. Consider a coefficient of harmonic linearization k_3 at like the matrix G_0 as:

$$G_0 = G + k_3\delta\kappa^T \tag{5}$$

which $\pm i\omega_0$ $(\omega_0 > 0)$ eigenvalues the matrix G_0 and the rest have negative real parts. We assume that such k_3 exists. Then, rewrite system 4 as follows:

$$\frac{\mathrm{d}x}{\mathrm{d}t} = G_0 x + \delta\rho(\kappa^T x), \tag{6}$$

where $\rho(\iota) = \Psi(\iota) - k_3\iota$. We introduce a fixed sequence of functions $\rho^0(\iota), \rho^1(\iota), \ldots, \rho^n(\iota)$ such that the graphs of the neighboring functions $\rho^i(\iota)$ and $\rho^{i+1}(\iota)$, $(i = 0, \ldots, n-1)$ partly disagree from each other.

Suppose that the function $\rho^0(\iota)$ is small, and $\rho^m(\sigma) = \rho(\iota)$. In this situation, the smallness of function $\rho^0(\iota)$ allows one to apply the method of harmonic linearization for the system

$$\frac{\mathrm{d}x}{\mathrm{d}t} = G_0 x + \delta\rho^0(\kappa^T x) \tag{7}$$

and determine a stable nontrivial periodic solution $x^0(t)$. In order to localize the attractor of system (5), put up the numerical transformation of this periodic solution. As we obtain the primary condition $x^0(0)$ of the periodic solution, system (7) can be changed by $H(X = HY)$ to the form:

$$\begin{cases} \dot{z_1} = -\omega_0 z_2 + v_1\rho^0(z_1 + c_3^T Z_3) \\ \dot{z_2} = \omega_0 z_1 + v_2\rho^0(z_1 + c_3^T Z_3) \\ \dot{Z_3} = A_3 Z_3 + V_3\rho^0(z_1 + c_3^T Z_3). \end{cases} \tag{8}$$

So z_1 and z_2 are scalar values; Z_3 is an $(n-2)$-dimensional vector, V_3 and c_3 are an $(n-2)$-dimensional vectors; v_1 and v_2 are real numbers; and A_3 is an $(n-2)\times(n-2)$ matrix, where all of its eigenvalues have negative real parts. Supposed that, for the matrix A_3, there exists $d_3 > 0$ such that

$$Z_3^T(A_3 + A_3^T)Z_3 \le -2d_3\,|Z_3|^2 \quad \forall Y_3 \in \mathbb{R}^{n-2}. \tag{9}$$

2.3 Poincare map for harmonic linearization in vector case

Define system (8) with $\phi = \varepsilon\rho$, where the parameter ε is (ε). Suppose, for the $\rho(z)$,

$$|\rho(z') - \rho(z'')| \le L|z' - z''| \quad \forall z', z'' \in \mathbb{R}^n \tag{10}$$

is satisfied. In a phase space of system (8), we introduce the following formula:

$$\Omega = \{|Z_3| \le M_\varepsilon, \quad z_2 = 0, z_1 \in [\lambda_1, \lambda_2]\}. \tag{11}$$

Hither, $M > 0$, $\lambda_1 > 0$, $\lambda_2 > 0$. Introduce n-dimensional vector $O_n(\varepsilon)$ as follows:

$$O_n(\varepsilon) = \begin{pmatrix} O(\varepsilon) \\ \vdots \\ O(\varepsilon) \end{pmatrix} \tag{12}$$

By using the conditions (10) and (8) for the solutions with initial data from Ω, we take out the formulas

$$\begin{cases} z_1(t) = \cos(\omega_0 t)z_1(0) + O(\varepsilon), \\ z_2(t) = \sin(\omega_0 t)z_1(0) + O(\varepsilon), \\ Z_3(t) = \exp(At)Z_3(0) + O_{n-2}(\varepsilon). \end{cases} \tag{13}$$

From relation (13), it follows that for any point $z_1(0)$, $z_2(0) = 0$, and $Z_3(0)$ belonging to Ω, exists a number

$$\Lambda = \Lambda(z_1(0), z_2(0)) = 2\pi/\omega_0 + O(\varepsilon) \tag{14}$$

such as relations

$$z_1(t) > 0, \quad z_2(t) = 0, \quad \forall t \in (0, \Lambda) \tag{15}$$

are not verified. Construct a Poincare map P of the list Ω for the trajectories of system (8):

$$P = \begin{Vmatrix} z_1(0), & z_1(T), \\ 0, & 0, \\ z_2(0). & z_2(T). \end{Vmatrix}. \tag{16}$$

Introduce the describing function Φ of a real variable ι as follows:

$$\Phi(\iota) = \left[\int_0^{2\pi/\omega_0} \rho_1(\cos(\omega_0 t)\iota), (\sin(\omega_0 t), 0)\cos(\omega_0 t) + \rho_2(\cos(\omega_0 t)\iota), (\sin(\omega_0 t), 0)\sin(\omega_0 t)\right]\mathrm{d}t. \tag{17}$$

From relation (13) and condition (10) for solutions of system (8), we obtain the following relations:

$$|y_3(\Lambda)| \le D_\varepsilon, \tag{18}$$

$$z_2^1(\Lambda) - z_2^1(0) = 2z_1(0)\varepsilon\Phi(z_1(0)) + O(\varepsilon^2). \tag{19}$$

Theorem 1. *If the inequalities*

$$\Phi(\iota_1) > 0, \quad \Phi(\iota_2) < 0 \tag{20}$$

are verified, then, for $\varepsilon > 0$, *we have*

$$P\Omega \subset \Omega. \tag{21}$$

From this theorem, and the Brouwer fixed point theorem, we have the following conclusions.

Theorem 2. *If the inequalities* (20) *are verified, then, for* $\varepsilon > 0$, *system* (8) *has a periodic solution with the period as follows:*

$$\Lambda = 2\pi / \omega_0 + O(\varepsilon). \tag{22}$$

This solution is stable in the sense that its neighborhood Ω *is mapped into itself*: $P\Omega \subset \Omega$.

Theorem 3. *If the conditions*

$$\Phi(\iota_0) = 0, \quad b_1 \frac{\mathrm{d}\Phi(\iota)}{\mathrm{d}\iota}\,|_{\iota=\iota_0} > 0 \tag{23}$$

are verified, then for $\varepsilon > 0$ *system with scalar nonlinearity has* Λ *periodic solution.*

2.3.1 Justification of hidden bifurcation in a 2D scroll via saturated function series (harmonic linearization method in vector case)

The Theorems 1–3 were proved that the positive parameter ι_0 is a solution for the function Φ to find a Poincare map [12].

The previous work [16] has proven a hidden bifurcation in multispirals generated by saturated function series, which is similar to the method introduced by Menacer et al. [14] for Chua multi-scroll attractors. In this work, we apply the above-described multi-step procedure for the localization of hidden bifurcation in vector case (Poincare map harmonic linearization), and we developed for study a hidden bifurcation in 2D scroll.

After a lot of calculation for our system (1–3), we found a field for the parameter ι_0 (the solution),

$$\iota_1 < \iota_0 < \iota_2 \tag{24}$$

in this field, we noted that the last three theorems are satisfied. For our system, we took $\iota_0 > 50$ and $\iota_0 < 10$ in this field and the function Φ has a solution.

3 Method for uncovering hidden bifurcations (2D scroll)

Theorem 2 can be used for looking hidden bifurcation with $n \times m$-grid scroll chaotic attractors generated via a saturated function series. In order to find a hidden bifurcation in a 2D scroll, the harmonic linearization coefficient, k_3, is essential. For this study, we rewrite the system 1–3 as follows:

$$\frac{\mathrm{d}x}{\mathrm{d}t} = Gx + \delta\Psi(\kappa^t x), \quad x \in \mathbb{R}^3 \tag{25}$$

Table 1: Numerical results of 2D hidden bifurcations for $p_1 = p_2 = 1$ and $q_1 = q_2 = 0$ (9 scroll)

Values of ε	0.55	0.7	0.75	0.82	0.85	0.93
Number of spirals	2	4	5	7	8	9

Here,

$$G = \begin{pmatrix} 0 & 1 & 0 \\ 0 & 0 & 1 \\ -a & -b & -c \end{pmatrix}, \quad \delta = \begin{pmatrix} 0 & -d_2/b & 0 \\ 0 & 0 & 1 \\ d_1 & d_2 & 0 \end{pmatrix}$$

$$\kappa = \begin{pmatrix} 0 & 1 & 0 \\ 1 & 0 & 0 \\ 0 & 1 & 0 \end{pmatrix}.$$

Define the coefficient k_3 and a small parameter ε, then system (25) can be rewritten as follows:

$$\frac{dx}{dt} = G_0 x + \delta \varepsilon \rho(\kappa^T x), \tag{26}$$

where

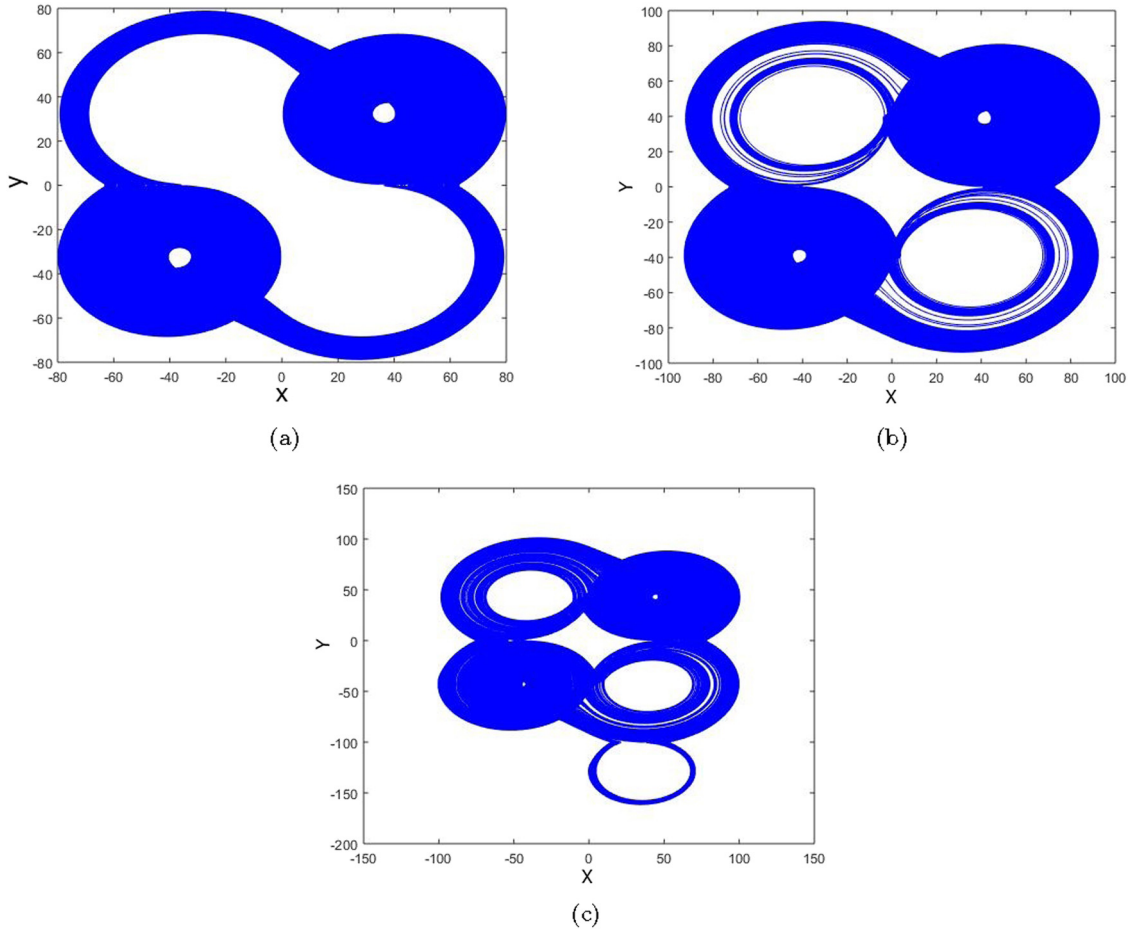

Figure 4: The increasing number of spirals of system (1-2-3) according to the increasing ε values, when $p_1 = p_2 = 1$ and $q_1 = q_2 = 0$ for nine scroll, $k_3' = 0.3$, $k = 50$, and $h = 100$. (a) Two spirals for $\varepsilon = 0.55$, (b) four spirals for $\varepsilon = 0.7$, and (c) five spirals for $\varepsilon = 0.8$.

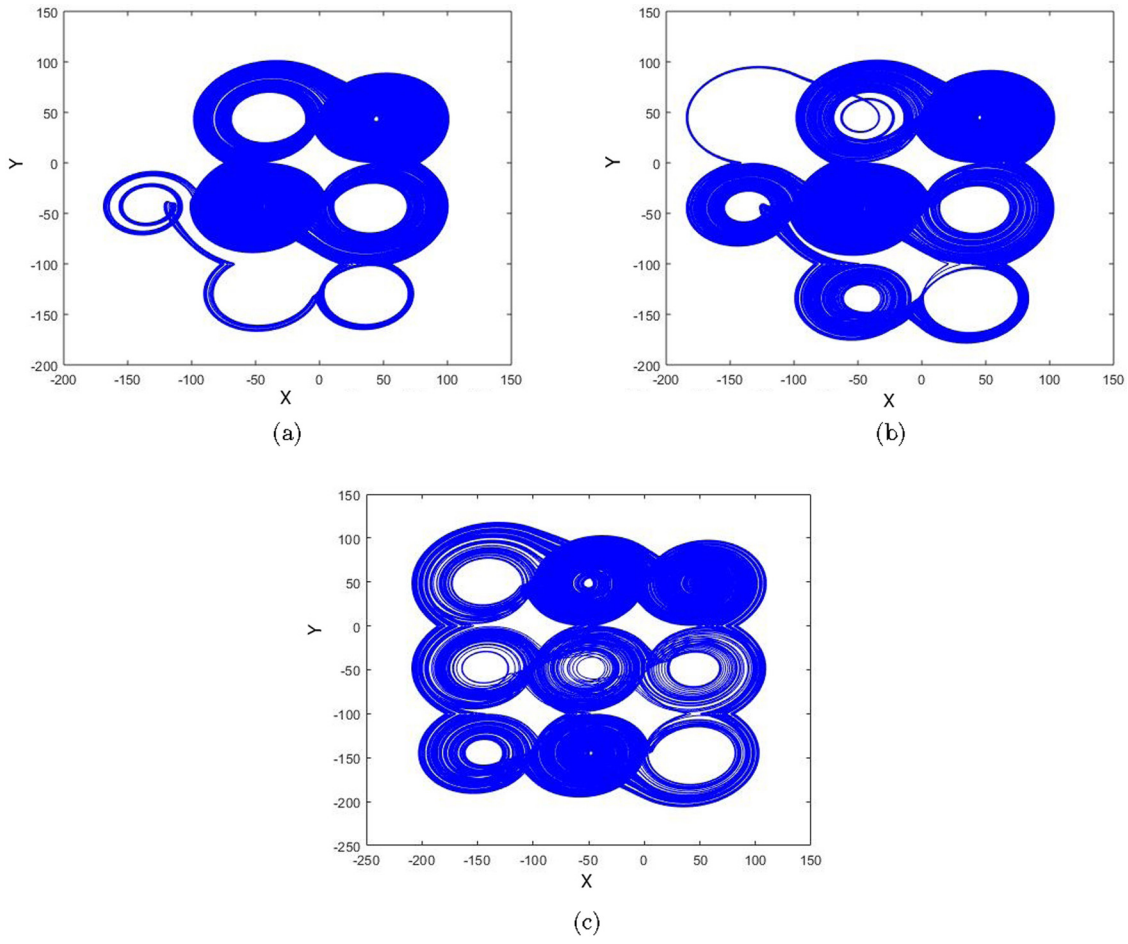

Figure 5: The increasing number of spirals of system (1-2-3) according to the increasing ε values, when $p_1 = p_2 = 1$ and $q_1 = q_2 = 0$ for nine scrolls $k_3' = 0.3$, $k = 50$, and $h = 100$. (a) Seven spirals for $\varepsilon = 0.82$, (b) eight spirals for $\varepsilon = 0.85$, and (c) nine spirals for $\varepsilon = 0.94$.

$$G_0 = G + k_3\delta\kappa^T = \begin{pmatrix} 1/bk_3d_2 & 1 & 1/bk_3d_2 \\ 0 & 0 & 1 \\ k_3d_1 - a & -b & k_3d_1 - c \end{pmatrix}.$$

The transfer function $W_G(s)$ of system (25) can be given as follows:

$$W_G(s) = \begin{pmatrix} 0 & \dfrac{a/d_2b - d_1s}{s^3 + cs^2 + bs + a} & \dfrac{-d_2s}{s^3 + cs^2 + bs + a} \\ 0 & \dfrac{(-d_2/b)s^2 - (c/b)s - d_2 - d_1}{s^3 + cs^2 + bs + a} & \dfrac{-d_2}{s^3 + cs^2 + bs + a} \\ 0 & \dfrac{a/d_2b - d_1s}{s^3 + cs^2 + bs + a} & \dfrac{-s_2}{s^3 + cs^2 + bs + a} \end{pmatrix}. \tag{27}$$

From this transfer function $W_G(s)$, the following starting frequency ω_0 and a coefficient of harmonic linearization k_3 are computed:

$$\omega_0 = 6.8, \quad k_3' = 0.3, \quad \text{and} \quad k_3'' = 0.17$$

3.1 Numerical result of hidden bifurcation in 2D scroll

The goal of this article is to study the hidden bifurcation in a 2D scroll, and we focused on the behavior of spirals when we took one value for coefficient harmonic linearization and two values for coefficient harmonic linearization for the solutions of system 26.

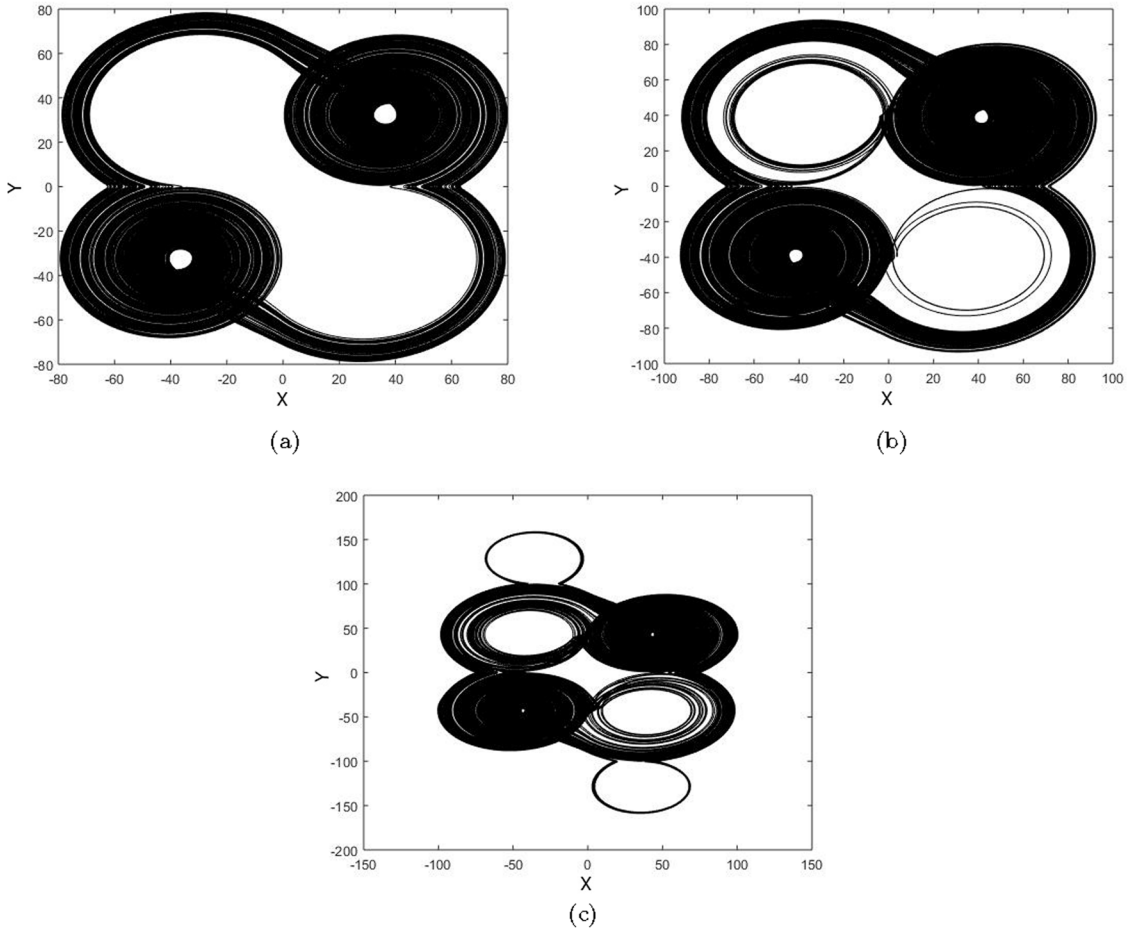

Figure 6: The increasing number of spirals of system (1-2-3) according to increasing ε values, when $p_1 = p_2 = 1$ and $q_1 = q_2 = 1$ for 16 scrolls, $k_3' = 0.3$, $k = 50$, and $h = 100$. (a) Two spirals for $\varepsilon = 0.55$, (b) four spirals for $\varepsilon = 0.7$, and (c) six spirals for $\varepsilon = 0.8$.

3.1.1 One value for coefficient harmonic linearization

In the first, we took one value for the coefficient of harmonic linearization k_3', so for $a = b = c = d_1 = d_2 = 0.7$, $k = 50$, $h = 100$ and taking $k_3 = 0.3'$. Then, the solutions of system 26 are calculated by increasing sequentially ε from the value $\varepsilon = 0.55$ to $\varepsilon = 1$, for $p_1 = p_2 = 1$, $q_1 = q_2 = 0$ for 9 scroll the initial conditions given by,

$$X^0(0) = -93.5056, \quad y^0(0) = 30.1536, \quad z^0(0) = 37.5733 \tag{28}$$

and for $p_1 = 1$, $p_2 = 1$, $q_1 = q_2 = 1$ for 16 scroll the initial conditions given by

$$X^0(0) = 51.2850, \quad y^0(0) = -63.5128, \quad z^0(0) = -8.2182. \tag{29}$$

Using these initial data, the procedure described above in Section 2 produces the values of the parameter ε at the bifurcation points where the attractor increases the number of spirals from 2 to 9 spirals (16 spirals, respectively), as shown in Table 1, in the following order: 2, 4, 5, 7, 8, and 9 (for 16 scroll, 2, 4, 6, 8, 10, 12, 14, and 16) depending on the values of ε, as shown in Figures 4–8.

Remark 1. In the case $p1 = p2 = 1$; $q1 = q2 = 1$, 16 scroll the apparition behavior of spirals is even (two by two) where the attractor increases the number of spirals from 2 to 16 spirals (2, 4, 6, 8, 10, 12, 14, 16), see Table 2 and Figures 6, 7, 8.

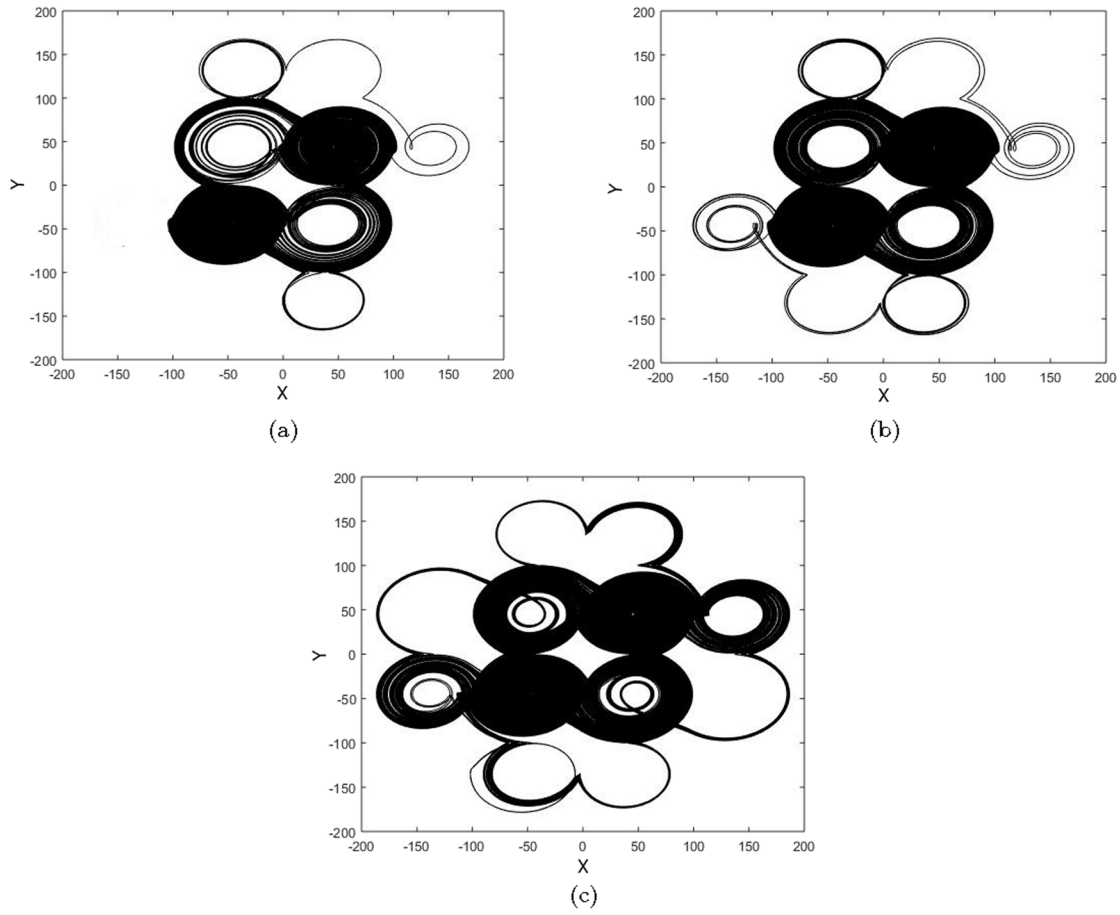

Figure 7: The increasing number of spirals of system (1-2-3) according to increasing ε values, when $p_1 = p_2 = 1$ and $q_1 = q_2 = 1$ for 16 scrolls, $k_3' = 0.3$, $k = 50$, and $h = 100$. (a) Eight spirals for $\varepsilon = 0.55$, (b) ten spirals for $\varepsilon = 0.829$, and (c) twelve spirals for $\varepsilon = 0.8$.

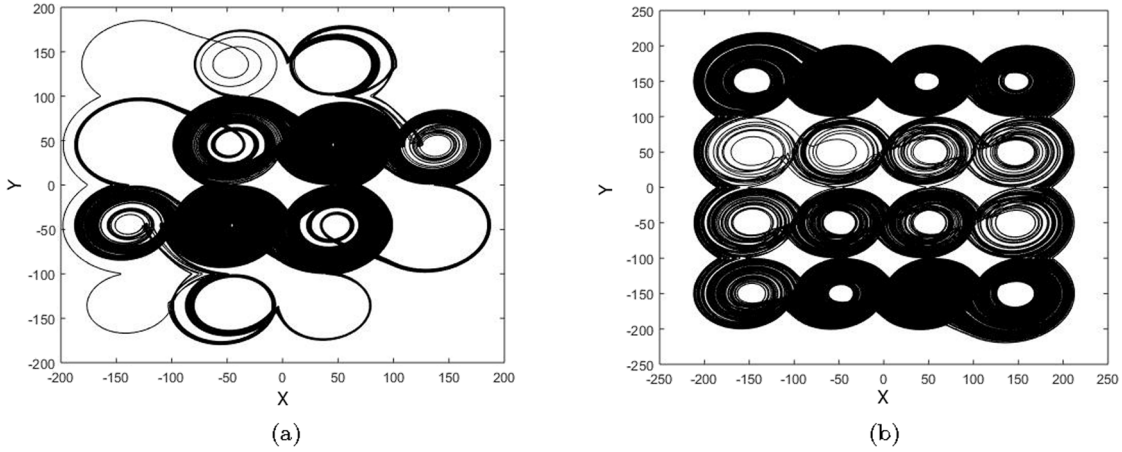

Figure 8: The increasing number of spirals of system (1-2-3) according to increasing ε values, when $p_1 = p_2 = 1$ and $q_1 = q_2 = 1$ for 16 scrolls, $k_3' = 0.3$, $k = 50$, and $h = 100$. (a) Fourteen spirals for $\varepsilon = 0.865$ and (b) 16 spirals for $\varepsilon = 0.94$.

Table 2: Numerical results of 2D hidden bifurcations for $p_1 = p_2 = 1$ and $q_1 = q_2 = 1$ (16 scrolls)

Values of ε	0.55	0.7	0.8	0.829
Number of spirals	2	4	6	8
Values of ε	0.83	0.86	0.865	0.94
Number of spirals	10	12	14	16

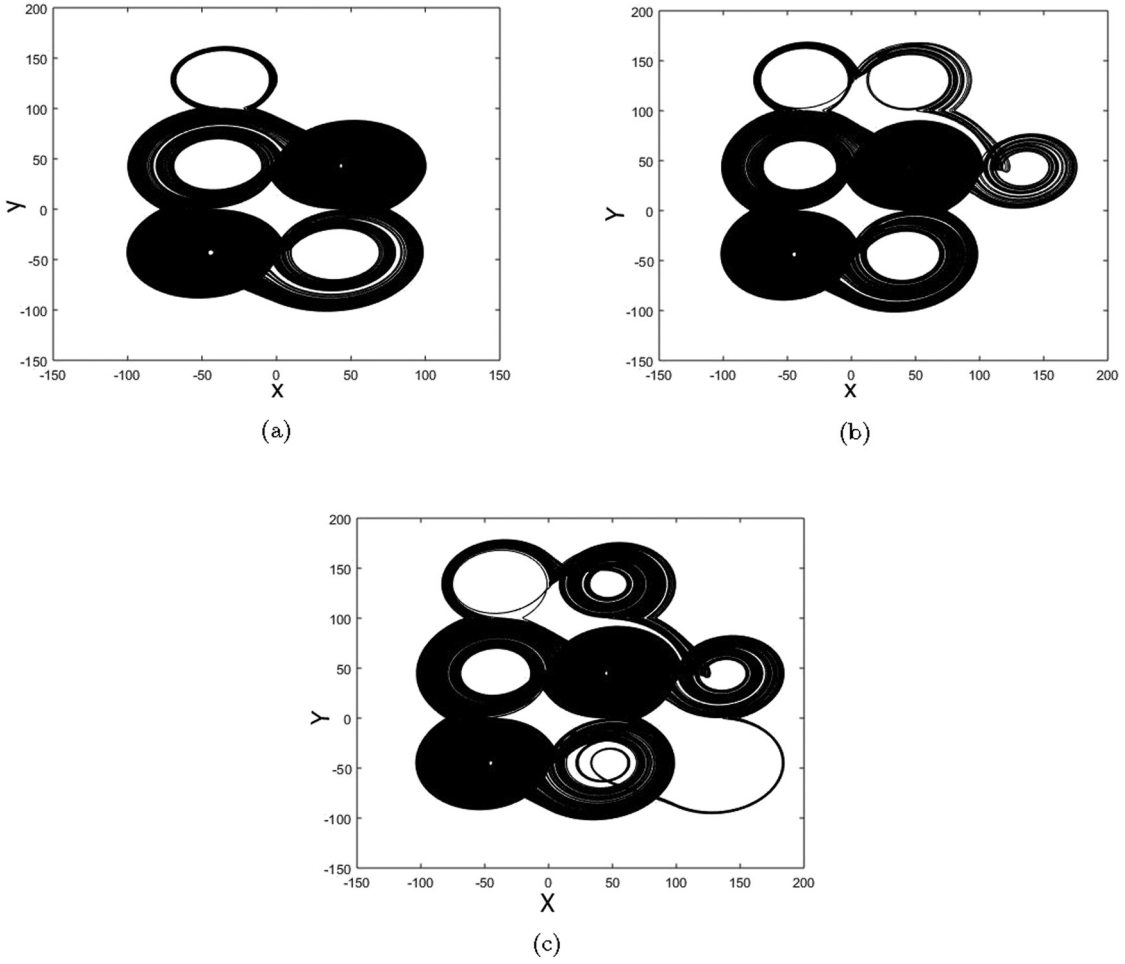

Figure 9: The increasing number of spirals of system (1-2-3) according to increasing ε values, when $p_1 = p_2 = 0$ and $q_1 = q_2 = 1$ for nine scrolls, $k_3' = 0.3$, $k = 50$, and $h = 100$. (a) Five spirals for $\varepsilon = 0.8$, (b) seven spirals for $\varepsilon = 0.82$, and (c) eight spirals for $\varepsilon = 0.85$, in symmetry with the increasing number of spirals according to increasing ε values, when $p_1 = p_2 = 1$ and $q_1 = q_2 = 0$.

Table 3: Numerical results of 2D hidden bifurcations for $p_1 = 1$, $p_2 = 1$, and $q_1 = q_2 = 1$ for the second case (16 scrolls)

Values of ε	0.55	0.85	0.867	0.873	0.9	0.915	1
Number of spirals	4	6	8	10	12	14	16

Remark 2. In the case $p1 = 0$, $q1 = 1$, $p2 = 0$, $q2 = 1$, the apparition behavior of spirals is different on the case(right) $p1 = 1$, $q1 = 0$, $p2 = 1$, $q2 = 0$, from these numerical results, it appears clearly that there exists some symmetry in the five, seven and eight spirals such as hidden bifurcation routes we studied in [16] see Figure 9.

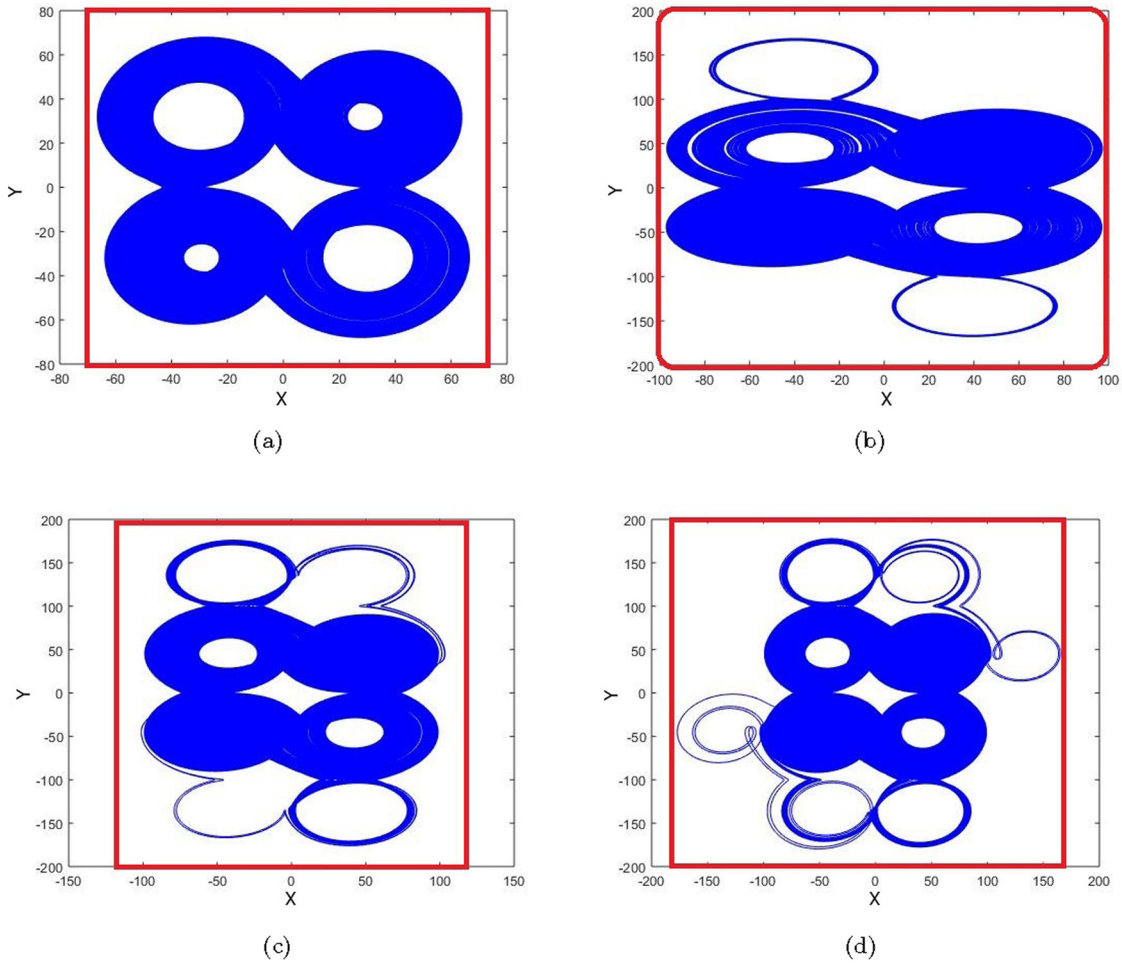

Figure 10: The increasing number of spirals of system (1-2-3) according to the increasing ε values, when $p_1 = p_2 = 1$ and $q_1 = q_2 = 1$ for 16 scrolls, $k_3' = 0.3$ and $k_3'' = 0.17$, $k = 50$, and $h = 100$. (a) Four spirals for $\varepsilon = 0.55$, (b) six spirals for $\varepsilon = 0.85$, (c) eight spirals for $\varepsilon = 0.867$, and (d) ten spirals for $\varepsilon = 0.873$.

3.1.2 Two values for coefficient harmonic linearization

We took two values of the coefficient of harmonic linearization k_3 where $k_3' = 0.3$ and $k_3'' = 0.17$, then, the solutions of system 26 are calculated by increasing sequentially ε from the value $\varepsilon = 0.55$ to $\varepsilon = 1$.

The results about the behavior of points bifurcations each spiral genesis in the cell (oblong) and the appearance of points bifurcation organized two-by-two-in all number of the scroll. For this purpose, we studied a 16 scroll for $p_1 = 1$, $p_2 = 1$, $q_1 = q_2 = 1$, we noted that the differences in the first spiral were that, in the first case, the first step (spiral) began with two spirals, whereas in the second case, the first step began with four spirals. The second difference in eight spirals is that, in the first case, the spiral number 8 has come up on top, not down as it is imposed, whereas in the second case, the appearance of two spirals to complete eight spirals is organized for building an oblong. The third difference in 14 spirals is that, in the first case, the behavior of two spirals from 12 to 14 spirals one up and then down just in the left side, whereas in a second case the behavior of two spirals from 12 to 14 spirals one up and then down in both sides (left and right), and we noted the other difference in values of ε, which is explained in Table 3 and Figures 10–14.

Remark 3. In our results, we noted that the coefficient harmonic linearization controlled the apparition behavior of hidden bifurcation, and in the case of two values for the coefficient harmonic linearization, we noted that it organized the apparition behavior of the hidden bifurcation better than the first case.

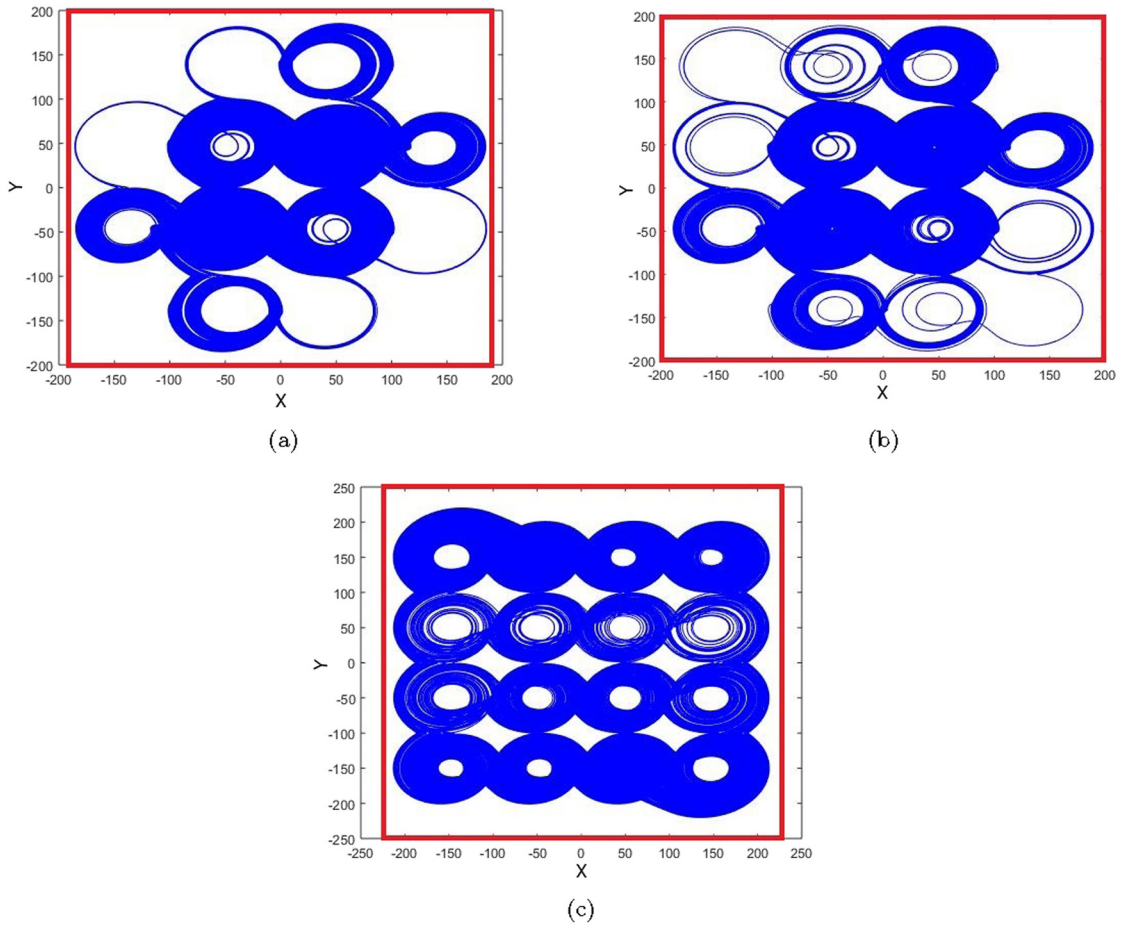

Figure 11: The increasing number of spirals of system (1-2-3) according to increasing ε values, when $p_1 = p_2 = 1$ and $q_1 = q_2 = 1$ for 16 scrolls, $k_3' = 0.3$, $k_3'' = 0.17$, $k = 50$, and $h = 100$. (a) Twelve spirals for $\varepsilon = 0.9$, (b) 14 spirals for $\varepsilon = 0.915$, and (c) 16 spirals for $\varepsilon = 0.96$.

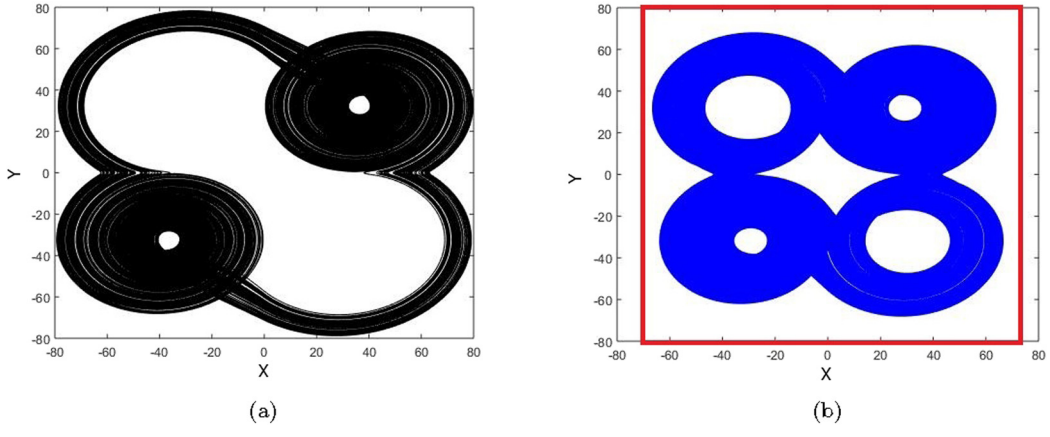

Figure 12: The comparison between the behavior of spirals of system (1-2-3) according to increasing ε values, when $p_1 = p_2 = 1$ and $q_1 = q_2 = 1$ for 16 scrolls in two cases. (a) Two spirals for $\varepsilon = 0.55$ for one value for coefficient harmonic linearization $k_3' = 0.3$ and (b) four spirals for $\varepsilon = 0.55$ for two values of coefficient harmonic linearization $k_3' = 0.3$ and $k_3'' = 0.17$.

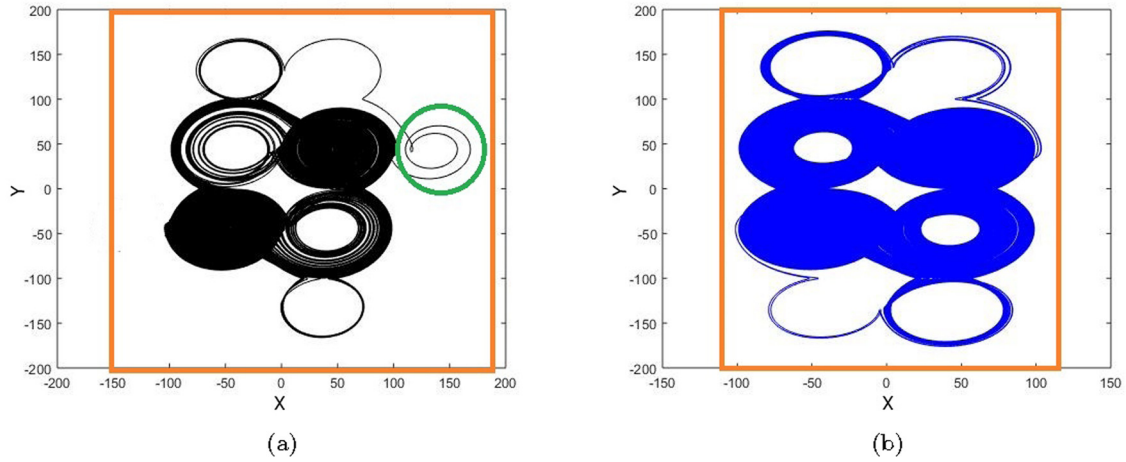

Figure 13: The comparison between the behavior of spirals of system (1-2-3) according to increasing ε values, when $p_1 = p_2 = 1$ and $q_1 = q_2 = 1$ for 16 scrolls in two cases. (a) Eight spirals for $\varepsilon = 0.829$ for one value of coefficient harmonic linearization $k_3' = 0.3$ and (b) eight spirals for $\varepsilon = 0.867$ for two values of coefficient harmonic linearization $k_3' = 0.3$ and $k_3'' = 0.17$.

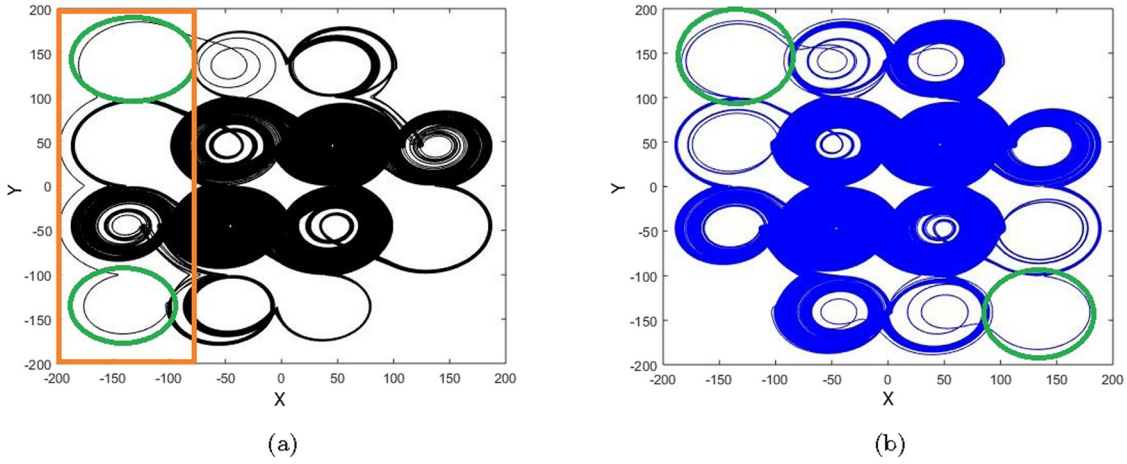

Figure 14: The comparison between the behavior of spirals of system (1-2-3) according to increasing ε values, when $p_1 = p_2 = 1$ and $q_1 = q_2 = 1$ for 16 scrolls in two cases. (a) Fourteen spirals for $\varepsilon = 0.865$ for one value of coefficient harmonic linearization $k_3' = 0.3$ and (b) 14 spirals for $\varepsilon = 0.915$ for two values of coefficient harmonic linearization $k_3' = 0.3$ and $k_3'' = 0.17$.

4 Conclusion

This article has initiated the behavior of hidden bifurcation in scroll via a saturated function series controlled by the coefficient harmonic linearization method, where a saturated function series approach is used for generating multi-scroll chaotic attractors, including 1D-scroll, 2D-grid scroll, and 3D-grid scroll attractors [9] from a given 1D-2D linear autonomic system with a saturated function series as the controller. In particular, a 2D Poincaré return map has been harshly structured to fulfill the chaotic behaviors of the double-scroll attractor. The method used is similar to the one presented by Leonov [10] and Leonov and Kuznetsov [11]. Such hidden bifurcations were first uncovered in 2016 for Chua multi-scroll attractors, which depend on a discrete parameter [14]. The novelties that this article introduces are (i) the model hidden bifurcation in a 2D scroll via saturated function series and (ii) controlling the behavior of a hidden bifurcation by the value of coefficient harmonic k_3.

Funding information: The authors state that there is no funding involved.

Author contributions: Zaamoune Faiza developed the code Matlab and simulations and wrote the article. Menacer Tidjani designed the experiments and corrected grammatical and stylistic errors.

Conflict of interest: The authors state no conflict of interest.

Informed consent: Informed consent has been obtained from all individuals included in this study.

Ethical approval: The conducted research is not related to either human or animals use.

Data availability statement: The datasets generated and/or analyzed during the current study are available from the corresponding author on reasonable request.

References

[1] J. Lü and G. Chen, *Generating multiscroll chaotic attractors: Theories, methods and applications*, Int J Bifurcat Chaos **16** (2006), no. 4, 775–858, DOI: https://doi.org/10.1142/S0218127406015179.

[2] X. Zhang and Ch. Wang, *A novel multi-attractor period multi-scroll chaotic integrated circuit based on CMOS wide adjustable CCCII*, IEEE Access **7** (2019), no. 1, 16336–16350, DOI: https://doi.org/10.1109/ACCESS.2019.2894853.

[3] H. Lin, Ch. Wang, Y. Sun, and T. Wang, *Generating n-scroll chaotic attractors from a memristor-based magnetized hopfield neural network*, IEEE Trans. Circuits Syst II Express Briefs **70** (2023), no. 1, 311–315, DOI: https://doi.org/10.1109/TCSII.2022.3212394.

[4] H. Lin, Ch. Wang, C. Xu, and X. Zhang, *A memristive synapse control method to generate diversified multi-structure chaotic attractors*, IEEE Trans Computer-aided Design Integrated Circuits Syst. **42** (2022), no. 3, 942–955, DOI: https://doi.org/10.1109/TCSII.2022.3186516.

[5] L. Zhou, Ch. Wang, and L. Zhou, *Generating hyperchaotic multi-wing attractor in a 4D memristive circuit*, Nonlinear Dyn. **85** (2016), no. 4, 2653–2663, DOI: http://dx.doi.org/10.10072Fs11071-016-2852-8.

[6] L. Zhou, Ch. Wang, and L. Zhou, *A novel no-equilibrium hyperchaotic multi-wing system via introducing memristor*, Int. J. Circuit Theory Appl. **46** (2018), no. 1, 84–98, DOI: https://doi.org/10.1002/cta.2339.

[7] Q. Deng and C. Wang, *Multi-scroll hidden attractors with two stable equilibrium points*, Chaos **29** (2019), no. 9, 093112, DOI: https://doi.org/10.1063/1.5116732.

[8] G. A. Leonov, N. V. Kuznetsov, and V. I. Vagaitsev, *Hidden attractor in smooth Chua systems*, Physica D **241** (2012), no. 18, 1482–1486, DOI: https://doi.org/10.1016/j.physd.2012.05.016.

[9] J. Lü, G. Chen, X. Yu, and H. Leung, *Design and analysis of multiscroll chaotic attractors from saturated function series*, IEEE Trans. Circuits Syst. **51** (2004), no. 12, 2476–2490, DOI: https://doi.org/10.1109/TCSI.2004.838151.

[10] G. A. Leonov, *Effective methods for periodic oscillations search in dynamical systems*, Appl. Math. Mech. **74** (2010), no. 1, 37–73, DOI: http://dx.doi.org/10.1016/j.jappmathmech.2010.03.004.

[11] G. A. Leonov and N. V. Kuznetsov, *Localization of hidden Chua's attractors*, Phys. Lett. A **375** (2011), no. 23, 2230–2233, DOI: https://doi.org/10.1016/j.physleta.2011.04.037.

[12] G. A. Leonov and N. V. Kuznetsov, *Analytical numerical methods for investigation of hidden oscillations in nonlinear control systems*, Proc. 18th IFAC World Congress, Milano, Italy **18** (2011), no. 1, 2494–2505, DOI: http://dx.doi.org/10.3182/20110828-6-IT-1002.03315.

[13] G. A. Leonov and N. V. Kuznetsov, *Hidden attractors in dynamical systems. From hidden oscillations in Hilbert-Kolmogrov, Aizerman, and Kalman problems to hidden chaotic attractor in Chua circuits*, Int. J. Bifurcat. Chaos **23** (2013), no. 1, 1330002–13300071, DOI: https://doi.org/10.1142/S0218127413300024.

[14] T. Menacer, R. Lozi, and L. O. Chua, *Hidden bifurcations in the multispiral Chua attractor*, *Int. J. Bifurcat. Chaos* **16** (2016), no. 4, 1630039–1630065, DOI: https://dx.doi.org/10.1142/S0218127416300391.

[15] X. Zhang and C. Wang, *Multiscroll hyperchaotic system with hidden attractors and its circuit implementation*, Int. J. Bifurcat. Chaos **29** (2019), no. 9, 1950117, DOI: https://doi.org/10.1142/S0218127419501177.

[16] F. Zaamoune, T. Menacer, R. Lozi, and G. Chen, *Symmetries in hidden bifurcation routes to multiscroll chaotic attractors generated by saturated function series*, J. Adv. Eng. Comput. **3** (2019), no. 4, 511–522, DOI: https://doi.org/10.1142/S0218127419501177.